

# Estimating larval fish growth under size-dependent mortality: a numerical analysis of bias

Tian Tian, Øyvind Fiksen, and Arild Folkvord

**Abstract:** The early larval phase is characterized by high growth and mortality rates. Estimates of growth from both population (cross-sectional) and individual (longitudinal) data may be biased when mortality is size-dependent. Here, we use a simple individual-based model to assess the range of bias in estimates of growth under various size-dependent patterns of growth and mortality rates. A series of simulations indicate that size distribution of individuals in the population may contribute significantly to bias in growth estimates, but that typical size-dependent growth patterns have minor effects. Growth rate estimates from longitudinal data (otolith readings) are closer to true values than estimates from cross-sectional data (population growth rates). The latter may produce bias in growth estimation of about  $0.03 \text{ day}^{-1}$  (in instantaneous, specific growth rate) or  $>40\%$  difference in some situations. Four potential patterns of size-dependent mortality are tested and analyzed for their impact on growth estimates. The bias is shown to yield large differences in estimated cohort survival rates. High autocorrelation and variance in growth rates tend to increase growth estimates and bias, as well as recruitment success. We also found that autocorrelated growth patterns, reflecting environmental variance structure, had strong impact on recruitment success of a cohort.

**Résumé :** Le début de la phase larvaire se caractérise par des taux élevés de croissance et de mortalité. L'estimation de la croissance à l'aide de données provenant de la population (transversales) et des individus (longitudinales) peut être faussée lorsque la mortalité est dépendante de la taille. Nous utilisons ici un modèle simple basé sur l'individu afin d'évaluer l'étendue de l'erreur dans les estimations de croissance sous divers patrons de taux de croissance et de mortalité reliés à la taille. Une série de simulations indique que la distribution en taille des individus dans la population peut contribuer significativement à l'erreur des estimations de croissance, mais que les patrons typiques de croissance dépendant de la taille n'ont que des effets mineurs. Les estimations de la croissance à partir de données longitudinales (lectures d'otolithes) sont plus près des valeurs réelles que les estimations à partir de données transversales (taux de croissance de la population). Ces dernières peuvent générer une erreur dans l'estimation de la croissance d'environ  $0,03 \text{ jour}^{-1}$  (taux spécifique instantané de croissance) ou une différence de  $>40\%$  dans certains cas. Nous testons quatre patrons potentiels de mortalité taille dépendante et analysons leur impact sur les estimations de croissance. Nous montrons que cette erreur produit d'importantes différences dans les estimations de taux de survie de la cohorte. Une autocorrélation et une variance importantes des taux de croissance ont tendance à faire augmenter les estimations de la croissance, l'erreur ainsi que le succès du recrutement. Nous observons également que les patrons de croissance autocorrélés, qui représentent la structure de la variance environnementale, ont un fort impact sur le succès du recrutement d'une cohorte.

[Traduit par la Rédaction]

## Introduction

The early life history of fish is characterized by high rates of mortality (Cushing 1975; Bailey and Houde 1989; Leggett and Deblois 1994). Survival of marine pelagic organisms (e.g., eggs and larvae) change with size: larger individuals typically have lower risk of mortality (Peterson and Wroblewski 1984; McGurk 1986). The "growth–mortality" hypothesis argues that faster-growing and -developing larvae are more likely to pass through each stage rapidly, thereby lowering the cumulated mortality during early stages (Bailey

and Houde 1989). Many fish species have allometric, dome-shaped specific growth rates, increasing during early ontogeny, leveling off, and eventually decreasing with size (Fonds et al. 1992; Folkvord 2005). The interaction between size-dependent growth and mortality affects the size distribution of larval survivors (Huston et al. 1988) and necessitates a distinction between population growth rates and true mean growth rates of individual fish (Ricker 1975), but it is known that bias is introduced when using mean values of population data under high mortality rates (e.g., Otterå 1992).

Received 22 June 2006. Accepted 13 December 2006. Published on the NRC Research Press Web site at <http://cjfas.nrc.ca> on 14 April 2007.  
J19381

T. Tian,<sup>1,2</sup> Ø. Fiksen, and A. Folkvord. Department of Biology, University of Bergen, P.O. Box 7800, 5020 Bergen, Norway.

<sup>1</sup>Corresponding author (e-mail: [tian.tian@gkss.de](mailto:tian.tian@gkss.de)).

<sup>2</sup>Present address: Institute for Coastal Research, GKSS Research Center, Max Planck Street 1, Building 11 (KOE), 21502 Geesthacht, Germany.

One way to estimate growth is to group discrete population samples and compare mean size of surviving fish at successive ages. This is termed “cross-sectional” data analysis for population growth rate. Such analysis assumes no size-biased sampling or mortality between sampling intervals (Ricker 1975). Alternatively, “longitudinal” data from otolith readings use individual growth trajectories of sampled larvae (Chambers and Miller 1995). However, longitudinal growth estimates of survivors from the same cohort sampled at different times will differ under significant size-dependent mortality as some size fractions are less likely to be included in subsequent samples. The classical example is when bias emerges as a result of size selection by a fishery (“Lee’s phenomenon”; Ricker 1975).

Given the absence of correction for size-dependent mortality in larval fish growth estimates, it is instructive to know under which conditions bias occurs. Both growth and mortality are highly nonlinear processes and the interactions between them are far from trivial. Huston and DeAngelis (1987) listed four critical factors responsible for changes in size distributions as individuals develop: (i) the initial size distribution; (ii) the distribution of growth rates among the individuals; (iii) the size and time dependence of the growth rate of each individual; and (iv) size-dependent mortality. Furthermore, short-term, small-scale environmental variability are expected to affect cohort survival rate (Letcher and Rice 1997; Pitchford and Brindley 2001; Pitchford et al. 2005), and thus the mean properties from population data may not accurately predict development and survival of fish populations (Rice et al. 1993; Gallego et al. 1996; Pepin 2004).

The many advantages of individual-based models (IBMs) in ecology have been discussed by various authors (Huston et al. 1988; DeAngelis and Gross 1992; Grimm and Railsback 2005). Here we use an IBM to trace growth and survival of a larval cohort through early life stages under various scenarios of size-dependent growth and mortality rates. Knowing the growth rates of survivors, we then estimate daily growth rates of the developing population with cross-sectional or longitudinal methods (Ricker 1975; Chambers and Miller 1995). The biases are obtained by comparing average growth rates of individuals at successive ages with the average growth rates of final survivors. The potential magnitudes and patterns of bias are evaluated according to three patterns or mechanisms of size-dependent mortality rate: (i) decreasing with size (Peterson and Wroblewski 1984; McGurk 1986); (ii) increasing with size (visual predation); and (iii) threshold size dependence in escape (e.g., gape-limited intracohort cannibalism). Two species with different allometric growth patterns (larval Atlantic cod (*Gadus morhua*) and Atlantic herring (*Clupea harengus*)) are chosen as model organisms. Cod larvae have a dome-shaped growth potential with size (Otterlei et al. 1999), whereas growth rate in larval herring is relatively independent of size (Fiksen and Folkvord 1999). We also investigate bias under variable and autocorrelated growth rates, which is anticipated for patchy environments, and how this environmental structure affects cohort survival in the model. In summary, we wish to determine (i) the magnitude of bias induced by using mean values of population data; (ii) how potential bias of growth varies with larval size, ini-

tial size distribution, and the allometric patterns of growth- and size-dependent mortality regimes; and (iii) the effects of environmental variability on larval survival and growth estimates.

## Materials and methods

The individual-based model is initialized with a cohort of 2-day-old yolk-sac larval cod. Population size declines dramatically as the result of size-dependent mortality, therefore the “super-individual” concept (Scheffer et al. 1995) is applied (grouping together many individuals with identical attributes). We let  $10^4$  super-individuals represent the larval cohort. Four attributes characterize each super-individual  $i$  over time: dry weight ( $DW_i$ , mg), standard length ( $SL_i$ , mm), probability of survival ( $PS_i$ ), and the number of identical individual survivors ( $N_i$ ) represented by each super-individual. (Appendix A defines all symbols used for growth estimates in the IBM.) Age is implicit as only a single cohort is traced. Simulations run until larvae reach an age of 60 days posthatch (DPH) in time steps of 1 h. Data of all super-individuals are stored once each day and compared with population assessments.

### Larval growth models

Daily growth (SGR, %·day<sup>-1</sup>) of larval Norwegian coastal cod (*Gadus morhua*) under optimal conditions in the lab is a function of dry body mass (DW, mg) and water temperature ( $T$ , °C) (Otterlei et al. 1999; Folkvord 2005):

$$(1) \quad \text{SGR}(T, DW) = 1.20 + 1.80T - 0.078T(\ln DW) - 0.0946T(\ln DW)^2 + 0.0105T(\ln DW)^3$$

Here, we keep the temperature fixed at 6 °C, and then this translates to a specific instantaneous growth rate  $g_{c,i}(DW_i)$  of larval cod  $i$  with body mass  $DW_i$ :

$$(2) \quad g_{c,i}(DW_i) = \ln \left[ \frac{\text{SGR}(6, DW_i)}{100} + 1 \right]$$

For herring-like species, instantaneous growth rate  $g_{h,i}$  is independent of size, and because temperature is fixed at 6 °C, growth is a constant (Fiksen and Folkvord 1999):

$$(3) \quad g_{h,i} = -0.024 + 0.012 \times 6 = 0.048$$

Environmental stochasticity in growth  $\tilde{g}_{c,i}(DW_i, t)$  was modeled as an autocorrelated process (Ripa and Lundberg 1996):

$$(4) \quad \tilde{g}_{c,i}(DW_i, t) = g_{c,i}(DW_i) + e_i(t) \sqrt{1 - \alpha^2}$$

$$e_i(t) = \alpha \cdot e_i(t-1) + \sigma \cdot n(0,1) \cdot \sqrt{1 - \alpha^2}$$

where  $t$  is time in hours ( $e_i$  was reset once each day),  $n(0,1)$  is a random number drawn from a standard normal distribution,  $\alpha$  is the autocorrelation coefficient ( $0 \leq \alpha \leq 1$ ), and  $\sigma$  is standard deviation (variance =  $\sigma^2$ ). The growth rate  $\tilde{g}_{c,i}(DW_i, t)$  was not allowed to exceed 50% of the expected growth rate at any age, or to be less than 0. Equation 4 is practical in generating variability into individual growth trajectories, with no ( $\alpha = 0$ ) or high autocorrelation ( $\alpha$  approach 1) in time. For larval fish, this mimics a situation where growth rates of individuals are influenced by a patchy environment resulting from patchy prey, temperature, or other environ-

mental factors affecting growth. Low autocorrelation would simulate a fine-grained environment in which the likelihood of switching between good and bad environments on short time scales is high. High autocorrelation mimics more coarse-grained environments, so that a larva in a good or bad environment is likely to remain in this condition for some time. The structure of the environment may have implications for emerging size distributions of larval cohorts through distribution of growth rates among individuals and, consequently, their survival probabilities and bias of growth estimates.

### Larval mortality rates

Mortality or predation rates of larval fish are typically highly size-dependent. If invertebrate predators are the dominating predators, risk of predation tends to decrease with size, but if visual predators are important, risk of predation may increase with size (Bailey and Houde 1989). Here, we have applied four basic models of changes in mortality rates with size, two empirical models in which mortality drops with size, one in which risk increases, and one that chops off the smaller fraction of the cohort every week.

The daily natural mortality rates  $M_p$  ( $\text{day}^{-1}$ ) of pelagic organisms are observed to be dependent on body mass (Peterson and Wroblewski 1984):

$$(5) \quad M_p = 5.3 \times 10^{-3} (10^{-3} DW)^{-0.25}$$

McGurk (1986) found mortality rates  $M_M$  ( $\text{day}^{-1}$ ) of fish eggs and larvae to be even more size-dependent:

$$(6) \quad M_M = 2.2 \times 10^{-4} (10^{-3} DW)^{-0.85}$$

Predation rate from fish  $M_f$  ( $\text{day}^{-1}$ ) is assumed to be an increasing function of larval SL if other factors such as light, larval behavior, or depth of occurrence are held constant (Fiksen et al. 2002):

$$(7) \quad M_f = 5.5 \times 10^{-4} SL^2$$

In some situations, such as during intensive cannibalism or predation from an abundant gape-limited predator, all larvae below a given size may be removed from the population. In some situations, this could generate strong bias in growth estimates (Folkvord 1997). We remove larvae shorter than the average body length from the population at weekly intervals and refer to this mortality as  $M_c$ . SL (mm) as a function of body mass is  $SL = \exp[2.296 + 0.277(\ln DW) - 0.005128(\ln DW)^2]$  for larval cod (Folkvord 2005) and  $SL = 4.76[\ln(10^3 DW) - 2.9]$  for larval herring (Fiksen and Folkvord 1999).

Given a size-dependent mortality rate  $M[DW_i(t)]$  (i.e.,  $M_p$ ,  $M_M$ ,  $M_f$ , or  $M_c$ ), the probability  $Ps_i(t)$  of surviving one day ( $\Delta t$ ) for each super-individual  $i$  depends on body mass and size dependency in mortality:

$$(8) \quad Ps_i(t) = e^{-M[DW_i(t)]\Delta t}$$

The number of individual survivors represented by each super-individual  $N_i$  will decrease with  $Ps_i(t)$ , such that each super-individual  $i$  represents fewer individuals over time. Super-individuals ( $10^4$  individuals) are followed (60 days), each initially representing  $10^6$  (cod-like growth pattern) or  $10^8$  individuals (herring-like growth pattern).

### Estimating population growth and defining bias

Population growth rate  $g_{cs}(t)$  at time  $t$  (= age of cohort) from cross-sectional methods is estimated by using mean weight of individual larvae at successive days (Folkvord 1997):

$$(9) \quad g_{cs}(t) = \frac{\ln \overline{DW}(t) - \ln \overline{DW}(t-1)}{\Delta t}$$

where  $\overline{DW}(t)$  and  $\overline{DW}(t-1)$  are the mean body sizes (mg dry weight) of all individuals at days  $t$  and  $t-1$  (time interval  $\Delta t = 1$  day) from

$$(10) \quad \overline{DW}(t) = \frac{\sum_{i=1}^{10000} DW_i(t) \cdot N_i(t-1) \cdot Ps_i(t)}{\sum_{i=1}^{10000} N_i(t-1) \cdot Ps_i(t)}$$

The total abundance  $\sum_{i=1}^{10000} N_i(t)$  at  $t$  differs from that at  $t-1$  as

some individuals die during this time interval as a result of size-dependent mortality. However, estimates of true mean growth rates (as defined by us) require initial and final mean weights from the same individuals (Fig. 1a). To follow the growth rates of survivors only, we first ran the model forward for 60 days, stored the size development of the final surviving larvae, and calculated what we defined as true daily mean growth rate  $g_{TMG}$ :

$$(11) \quad g_{TMG}(t) = \frac{\sum_{i=1}^{10000} N_i(60) \cdot g_i(DW_i, t)}{\sum_{i=1}^{10000} N_i(60)}$$

With longitudinal data, the use of otoliths can yield information about individual growth trajectories that reflect true growth rates of survivors from samples at time  $t+1$ :

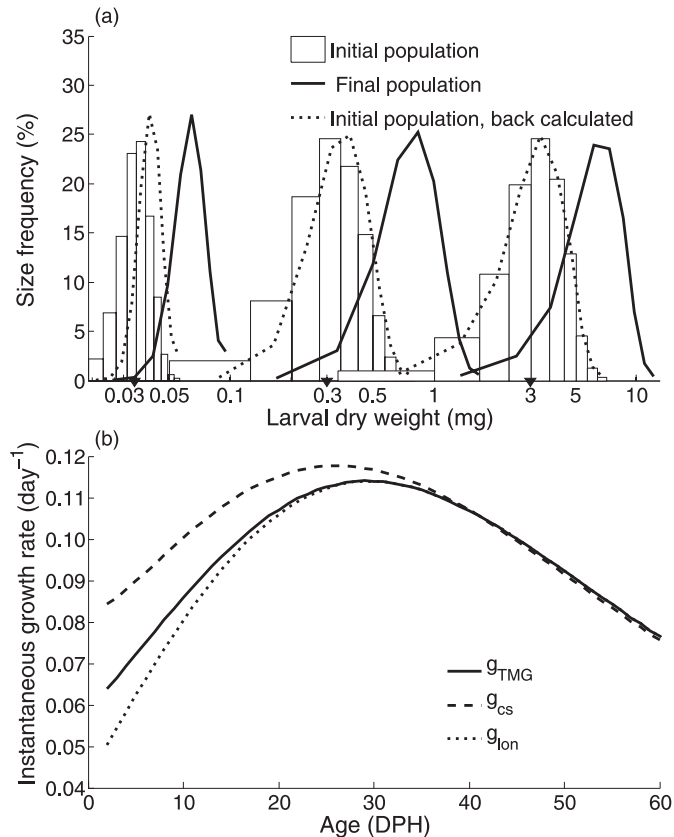
$$(12) \quad g_{lon}(t) = \frac{\sum_{i=1}^{10000} N_i(t+1) \cdot g_{c,i}(DW_i, t)}{\sum_{i=1}^{10000} N_i(t+1)}$$

However, a sample of individuals from any time (or cohort age)  $t$  ( $2 < t < 60$  DPH in the model) will give different growth histories compared with the final cohort under size-dependent mortality. This is because the final sample will consist of a size-biased subsample of all previous samples. We define bias inherent in longitudinal estimates as the difference in growth at age between a sample of survivors at 60 DPH and any sample from  $t < 60$  DPH. Technically, the bias from cross-sectional  $\epsilon_{cs}$  or longitudinal  $\epsilon_{lon}$  data (Fig. 1b) is given by

$$(13) \quad \epsilon_{cs} = g_{cs} - g_{TMG} \quad \text{and} \quad \epsilon_{lon} = g_{lon} - g_{TMG}$$

Note that there will be no bias in any estimate if mortality is not dependent on larval size (constant mortality rate).

**Fig. 1.** (a) Illustration of the bias induced by size-dependent mortality and cross-sectional data with a sampling interval of 1 week. The bars represent three different initial populations, and the solid lines represent the second sample (i.e., final population). Dotted lines represent the size frequency of individuals back-calculated from the second samples assuming no mortality. Solid triangles on the abscissa indicate the average weight (0.034, 0.3, and 3.0 mg dry weight) of initial populations, and the y axis represents larval size frequency in population biomass. (b) The instantaneous growth rate ( $\text{day}^{-1}$ ) estimated from cross-sectional or longitudinal data (continuously sampled) and the true mean growth rate back-calculated from 60 DPH.



### Overview of simulations

Unless specified otherwise, the initial dry weight of each super-individual is a normal deviate from a size distribution with mean dry weight ( $\pm$  standard deviation, SD) of  $0.034 \pm 0.006$  mg (restricted downwards to 0.02 mg) as in the rearing experiment of Otterlei et al. (1999). As a standard, the growth pattern is dome-shaped with size (eq. 1), temperature is fixed at 6 °C, the mortality rate  $M_M$  from McGurk (1986) is used, and bias is given from cross-sectional assessment, with sampling intervals of 1 day.

We investigated the following potential candidates for bias in growth estimates.

#### Experiment 1: initial size distribution

We simulated growth estimates using initial body sizes from a normal ( $0.034 \pm 0.006$  mg) and a uniform ( $0.034 \pm 0.01$  mg) distribution with a fixed coefficient of variation

(CV) of 17%. Cohort variance in weight distribution develops naturally from growth and mortality processes.

#### Experiment 2: initial body size and size variability

We initiated 10 cohorts with increasing mean weights (i.e., 0.034, 0.05, 0.1, 0.3, 0.5, 1.0, 3.0, 5.0, 10.0, and 30.0 mg). The cohorts were given CVs either fixed at 17% (populations were regenerated at each size category) or emerging naturally from a developing cohort. The estimated emergent CVs for each cohort in this case were 17%, 24%, 32%, 39%, 41%, 41%, 38%, 35%, 31%, and 24%, respectively. In this case, bias is obtained by comparing the population growth rate at 1-week intervals, and each cohort is assessed only once to mimic discrete sampling in the field.

#### Experiment 3: growth pattern

We simulated one cohort with dome-shaped growth rates ( $g_c$ , eq. 2) and one with constant specific growth rates ( $g_h$ , eq. 3) starting from the same initial population.

#### Experiment 4: size-dependent mortality rate

Each mortality model ( $M_M$ ,  $M_P$ ,  $M_f$ , and  $M_C$ ) was assessed for effects on bias.

#### Experiment 5: demographic and environmental stochasticity

The stochasticity parameters  $\alpha$  and  $\sigma$  (eq. 4) were varied and both bias and recruitment success were compared with deterministic simulations.

## Results

#### Experiment 1: initial size distribution

Bias decreases near exponentially with age for both normal and uniform initial size distributions (Fig. 2a). A uniformly distributed larval cohort is more biased initially, but the normally distributed cohort becomes more biased after about 1 week. The maximal bias of  $0.027 \text{ day}^{-1}$  is about 40% of the true mean growth rate of  $0.06 \text{ day}^{-1}$ , but the bias decreases to less than  $0.01 \text{ day}^{-1}$  within 10 days.

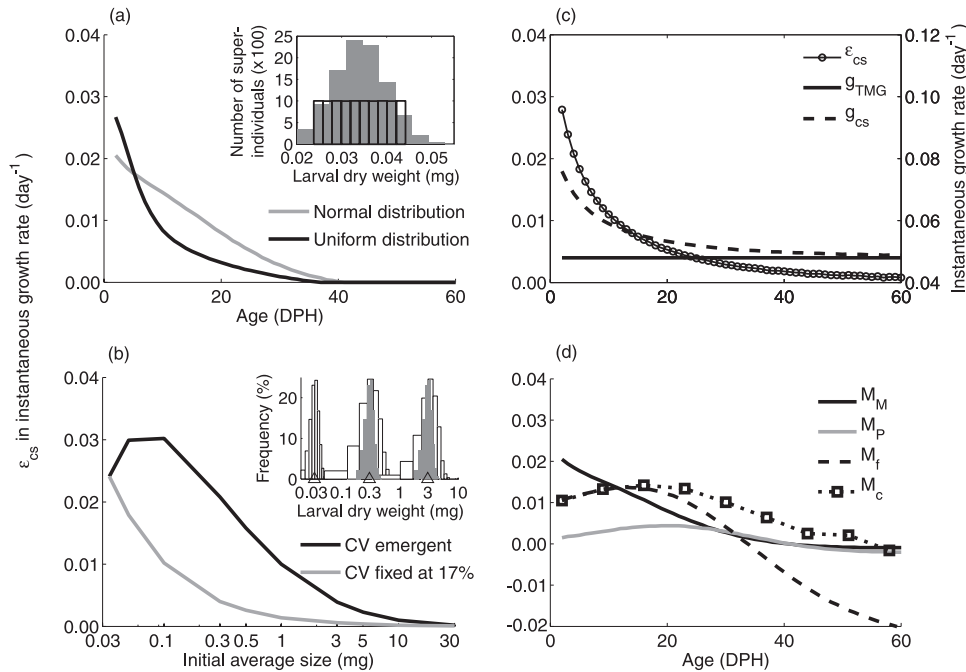
#### Experiment 2: initial body size and size variability

For initial populations of increasing average weight but constant CV of 17%, bias peaks at  $0.024 \text{ day}^{-1}$  and decreases exponentially with weight (Fig. 2b). For initial populations with varying CVs, bias peaks at around 0.1 mg ( $0.03 \text{ day}^{-1}$ ). The size variation increases from 17% of the first initial population (smallest average size) to 32% of the third initial population owing to the dome-shaped growth pattern. The CV peaks (41%) at 0.5–1.0 mg, but the bias of growth estimates declines before this because mortality rate drops with weight and supersedes the effect of increasing variance. The mean body size of the initial population has some influence owing to the size-specific mortality function  $M_M$ , but the main factor generating biased estimates is weight variability of initial population (i.e., CV).

#### Experiment 3: growth pattern

When applying a size-independent growth rate (Fig. 2c), the constant CV of the size distribution will be preserved (as in experiment 2) and growth estimates are biased only by

**Fig. 2.** Bias ( $\epsilon_{cs}$ , in terms of specific growth per day, see eq. 13) induced by size-dependent mortality estimated in four numerical experiments. (a) Experiment 1: bias with different initial length distributions, uniform (solid line) and normally distributed (shaded line), respectively. The initial populations are illustrated in the inset: uniform distribution (open bars) and normal distribution (shaded bars). (b) Bias depending on mean weight of initial populations and initial size distribution. The CV of the initial populations is either constant (start populations are reset at each mean size (shaded line)) or varying (CVs emerge from cohort development (solid line)). Bars in the inset illustrate 3 of 10 initial populations with constant (shaded bars) or varying (open bars) CVs, respectively. (c) True and estimated growth rate and bias ( $\text{day}^{-1}$ ) for larvae with constant growth ( $g_h$ ) and size-dependent mortality  $M_M$ . (d) Bias in growth estimate from four models of size-dependent mortality rate ( $M_M$ ,  $M_P$ ,  $M_f$ , and  $M_c$ ).



size-dependent mortality rate. The maximal bias for constant growth is  $0.028 \text{ day}^{-1}$  compared with the true growth rate of  $0.048 \text{ day}^{-1}$ . This suggests that initial size distribution is more important than growth pattern when the size-dependent mortality rate is high.

#### Experiment 4: size-dependent mortality regimes

Estimates of growth rates are sensitive to the pattern of size-dependent mortality (Fig. 2d). The mortality model  $M_M$  can yield population growth rates  $0.02 \text{ day}^{-1}$  above true values, whereas the weaker size dependence from the Peterson and Wroblewski (1984) model  $M_P$  give almost no bias. Visual predators are positively size selective, producing an underestimation of growth rate that is negligible when larvae are small but more evident as the larvae grow. The initial positive bias under visual predation is a result of the dome-shaped (initially increasing) growth pattern with size. Gape-limited selection for the smallest larvae is simulated by culling larvae shorter than average length from the population weekly. The maximum bias is still less than  $0.02 \text{ day}^{-1}$ .

#### Experiment 5: demographic stochasticity and environmental grain

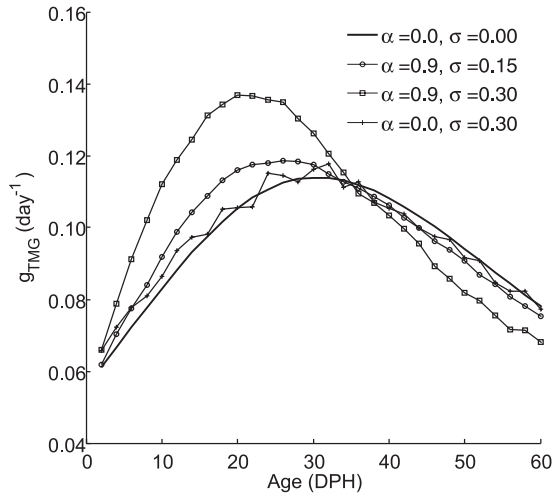
Here we test effects on growth estimates from varying the autocorrelation coefficient  $\alpha$  and variance  $\sigma^2$ . Generally the inclusion of stochasticity leads to similar maximum magnitudes of bias as in the deterministic case ( $\leq 0.02 \text{ day}^{-1}$ ). However, stochasticity itself changes both estimated popula-

tion growth rates and true mean growth rates. With no autocorrelation ( $\alpha = 0$ ), the survivors grow similarly to those in the deterministic growth pattern (Fig. 3). With autocorrelation, both estimated population growth rates and true mean growth rates increase above deterministic values, and consequently, the dome-shaped growth patterns peak earlier (Fig. 3). High autocorrelation ( $\alpha = 0.9$ ) and higher variance ( $\sigma^2$ ) allow some individuals to be more lucky initially and grow at high rates in the early phase with correspondingly high probability to be among the final survivors (Fig. 4). With strong size dependence in mortality, environmental stochasticity, and temporal autocorrelation (coarse-grained environments), survivors are those entrained in favorable environments in the early larval phase. This higher growth rate will shift up the size distribution of the cohort and lead to lower growth at higher ages owing to the dome-shaped growth pattern.

#### Implications of growth and mortality rates for cohort development

What is the implication of using biased (population estimates) rather than true growth rates (individual survivors) to assess cohort success? Applying the biased rather than the true rates of growth could cause two or more orders of magnitude differences in numbers reaching a given size (Table 1), or one order of magnitude difference when size-dependent mortality rate  $M_M$  is reduced by 10%. The importance of rapid growth in lowering cumulated mortality (e.g.,

**Fig. 3.** True mean growth rate ( $\text{day}^{-1}$ ) of 60 DPH larval cod under three simulated stochastic environments (lines with symbols) compared with the deterministic model (solid line). Autocorrelation and variance in the environment reflects the degree of patchiness in the environment. Note that growth rates feed back on the size structure at age, which then feeds back on growth rates because of the dome-shaped growth pattern with size; therefore relatively high growth rate at early age necessarily leads to lower growth rates at higher age.



Chambers and Trippel 1997) is also clear from this example. Applying  $M_M$  leaves only 7 survivors of  $10^{10}$  after 48 days (Table 1), whereas  $M_P$  leaves  $10^9$  individuals.

**Environmental variance structure and recruitment success**

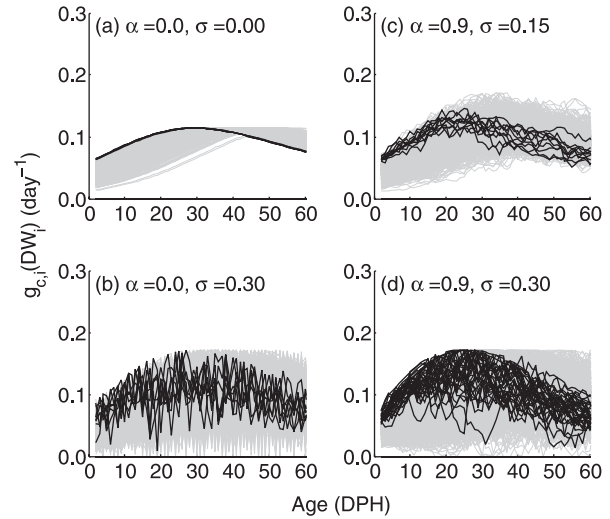
How will environmental variance structure affect larval survival? How important is the variability experienced in growth conditions between individuals for recruitment? The individual growth trajectories of survivors (Fig. 4) illustrate the importance of rapid growth in early life. Using the standard version of the model, we evaluate recruitment success as the number of surviving individual larva reaching 3.0 mg dry weight under different stochasticity schemes (autocorrelation and variance in growth determined by sets of parameters  $\alpha$  and  $\sigma^2$ ). Recruitment increases markedly with autocorrelation when  $\sigma > 0.3$  and with  $\sigma$  when  $\alpha > 0.4$  (Fig. 5). Generally, higher autocorrelation and variance leads to higher recruitment.

**Discussion**

The correction for size-dependent mortality in growth estimation, whether in the laboratory or field, is important but difficult to carry out in practice. It is therefore essential to know the magnitude and pattern of bias and to understand which factors and methods could generate biased estimates from data analysis. This study aims not to predict the exact errors involved in field or enclosures studies, but rather to theoretically explore the mechanisms under which the potential bias is likely to be significant.

Our results confirmed that growth estimates from individual-based longitudinal data are more accurate than rates obtained from cross-sectional data. However, it is important to

**Fig. 4.** Growth rate trajectories of 1000 super-individuals (shaded lines) of the cohort and the final survivors (solid lines) after 60 DPH for four scenarios: (a)  $\alpha = 0.0$  and  $\sigma = 0.0$ , five super-individuals survived; (b)  $\alpha = 0.0$  and  $\sigma = 0.30$ , eight super-individuals survived; (c)  $\alpha = 0.9$  and  $\sigma = 0.15$ , 10 super-individuals survived; (d)  $\alpha = 0.9$  and  $\sigma = 0.30$ , 32 super-individuals survived.



realize that even longitudinal estimates (e.g., otolith-based) can be biased when mortality rate is size-dependent. Significant bias is most likely to occur during the first 30 days of larval life. Estimates of growth rate may vary considerably depending on the initial size distribution. In particular, special attention should be paid to size distribution of similar-aged groups of small larvae when cross-sectional data are used to estimate growth (Folkvord et al. 1994). Allometric growth patterns did not affect growth estimates. Generally, the lower the growth rates of individuals, the higher is the bias induced by higher mortality rates. Based on our results, we recommend that ecological interpretations of differences less than  $0.03 \text{ day}^{-1}$  in estimated specific growth rates of larval fish be treated with caution as these differences can arise from estimation bias alone.

The model predicts that autocorrelated growth rates at the level of individuals will increase recruitment success. Some investigations report that prey species of larval fishes exhibit strong patchiness at spatial scales ranging from tens of kilometres to less than 10 m (e.g., Currie et al. 1998; Tokarev et al. 1998). It has been discussed for some time that prey patchiness may have a large effect on individual growth rates of fish larvae by causing variable encounter rates with prey over time, which could therefore have a wide range of effects on individual and cohort survival, depending on the scale and the intensity of patchiness and how the larval individuals react in the field (Pitchford and Brindley 2001; Pitchford et al. 2003; Pepin 2004). Individual growth both in otoliths and length are observed with significant serial autocorrelation (Folkvord et al. 2000; Pepin et al. 2001). The importance of environmental variability (e.g., temperature, food concentration, light, and turbulence) in regulating cohort survival rate has also been demonstrated in simulation studies (Gallego and Heath 1997; Letcher and Rice 1997;

**Table 1.** Recruitment variability predicted from true mean growth rate (TMG) (dome-shaped growth pattern), biased estimates, and various mortality formulations.

Growth rate (day <sup>-1</sup> )	Mortality rate (day <sup>-1</sup> )	Stage duration as recruits (days)	No. of recruits
$g_{\text{TMG}}^*$	$1.0 \times M_M$	48	7
$g_{\text{TMG}}^*$	$0.9 \times M_M$	48	59
$g_{\text{TMG}} + \epsilon_{\text{cs}}^\dagger$	$1.0 \times M_M$	42	1 302
$g_{\text{TMG}} + \epsilon_{\text{cs}}^\dagger$	$0.9 \times M_M$	42	6 357
$g_{\text{TMG}} + \epsilon_{\text{cs}}^\ddagger$	$1.0 \times M_M$	38	12 245
$g_{\text{TMG}} + \epsilon_{\text{cs}}^\ddagger$	$0.9 \times M_M$	38	47 769

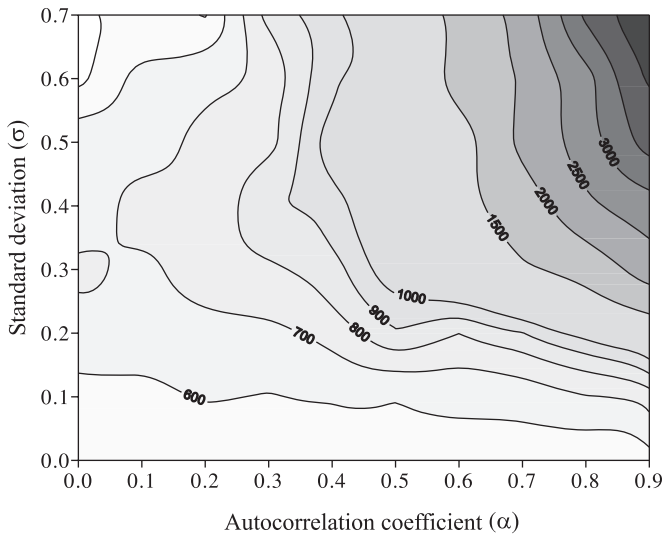
**Note:** Average initial size is 0.034 mg dry weight for 10<sup>10</sup> individuals and recruitment is defined as the number of surviving individuals reaching 3.0 mg dry weight. Stage duration: time to reach 3.0 mg dry weight as recruits.

\*Model from Folkvord (2005); see eqs. 1 and 2.

†Biased growth rate from a cohort with normal initial size distribution (Fig. 2a).

‡Biased growth rate from discrete samples with varying CVs (Fig. 2b).

**Fig. 5.** Recruitment variability related to environmental stochasticity and spatial-temporal structure. Recruitment is defined as the total number of individual survivors up to 3.0 mg dry weight as predicted by the standard version of the model in all cases of stochastic schemes (experiment 5). The number of survivors in the deterministic case is 561.



Lough et al. 2005). Gallego et al. (1996) suggest that daily growth variation in length are likely to reflect changes in the growth environment more closely during the larval stage because of relative low amounts of reserves and that small-scale spatial and temporal environmental variability in food availability influenced by, e.g., turbulence or light could be more important for larval survival than large-scale variation.

Our more abstract model confirms this general result and shows clearly how environmental variability structure may generate deviations between the survivors and the average individual. An implication is that the environmental variability will increase growth rate of survivors relative to the average individual under size-dependent mortality (Gallego and Heath 1997; Pepin et al. 2001; Dower et al. 2002). We simulated the relative scale between an individual and a patch by the autocorrelation coefficient. Low autocorrelation implies

that patchiness is so small that individuals frequently switch between good and bad conditions. Higher autocorrelation will keep individuals in good or bad environments over longer times, sorting out clear winners and losers, where winners will be fast-growing larvae with high chance of survival.

Accurate estimates of both growth and mortality rates are necessary to evaluate causes of recruitment failure and success in larval fish (Ricker 1975; Buckley et al. 2000; Govoni 2005). Back-calculation based on otolith readings offers greater potential accuracy than traditional techniques (Campana 1990; Anderson 1995). Besides, otolith techniques make the trajectories of fish early life history identifiable individually and then provide critical means to determine whether mortalities are at random or not (Chambers and Miller 1995). However, as Suthers et al. (1999) and Folkvord et al. (2000) pointed out, the precision of otolith growth history determination is restricted to periods with increment widths above 1–2  $\mu\text{m}$ . In several species in the temperate waters, larval growth in the first 2–3 weeks posthatch is characterized by increments around 1  $\mu\text{m}$ , which leads to the inaccuracy of mean growth rate estimated by individual-level historical growth in the field (Pepin et al. 2001).

An interesting topic for the future will be to make our model spatially explicit to further increase the understanding of spatially and temporally patchy environmental effects (e.g., frontal zones, prey patchiness, and temperature variability on various scales) on larval growth and survival and to quantify autocorrelation coefficients and the variance of stochastic factors relevant to individual larval growth in the field. Such analyses could also cast some light on potential benefits of extensive spawning periods, batch spawning, or the selection of spawning grounds in a variety of fishes.

## Acknowledgements

This is a contribution to GLOBEC Norway, ECOBE. T. Tian was funded by the Erasmus Mundus Programme, and Ø. Fiksen and A. Folkvord acknowledge the Norwegian Research Council for financial support. The manuscript benefited from comments made by two anonymous reviewers.

## References

- Anderson, C.S. 1995. Calculating size-dependent relative survival from samples taken before and after selection. *In* Recent developments in fish otolith research. *Edited by* D.H. Secor, J.M. Dean, and S.E. Campana. University of South Carolina Press, Columbia, S.C. pp. 455–466.
- Bailey, K.M., and Houde, E.D. 1989. Predation on eggs and larvae of marine fishes and the recruitment problem. *Adv. Mar. Biol.* **25**: 1–83.
- Buckley, L.J., Lough, R.G., Peck, M.A., and Werner, F.E. 2000. Comment: larval Atlantic cod and haddock growth models, metabolism, ingestion, and temperature effects. *Can. J. Fish. Aquat. Sci.* **57**: 1957–1960.
- Campana, S.E. 1990. How reliable are growth back-calculations based on otoliths. *Can. J. Fish. Aquat. Sci.* **47**: 2219–2227.
- Chambers, R.C., and Miller, T.J. 1995. Evaluating fish growth by means of otolith increment analysis: special properties of individual-level longitudinal data. *In* Recent developments in fish otolith research. *Edited by* D.H. Secor, J.M. Dean, and S.E. Campana. University of South Carolina Press, Columbia, S.C. pp. 155–175.
- Chambers, R.C., and Trippel, E.A. 1997. Early life history and recruitment in fish populations. Chapman and Hall Ltd., London, UK.
- Currie, W.J.S., Claereboudt, M.R., and Roff, J.C. 1998. Gaps and patches in the ocean: a one-dimensional analysis of planktonic distributions. *Mar. Ecol. Prog. Ser.* **171**: 15–21.
- Cushing, D.H. 1975. Marine ecology and fisheries. Cambridge University Press, Cambridge, UK.
- DeAngelis, D.L., and Gross, L.J. 1992. Individual based models and approaches in ecology: concepts and models. Routledge, Chapman and Hall, New York.
- Dower, J.F., Pepin, P., and Leggett, W.C. 2002. Using patch studies to link mesoscale patterns of feeding and growth in larval fish to environmental variability. *Fish. Oceanogr.* **11**: 219–232.
- Fiksen, Ø., and Folkvord, A. 1999. Modelling growth and ingestion processes in herring *Clupea harengus* larvae. *Mar. Ecol. Prog. Ser.* **184**: 273–289.
- Fiksen, Ø., Aksnes, D.L., Flyum, M.H., and Giske, J. 2002. The influence of turbidity on growth and survival of fish larvae: a numerical analysis. *Hydrobiologia*, **484**: 49–59.
- Folkvord, A. 1997. Ontogeny of cannibalism in larval and juvenile fish with special emphasis on Atlantic cod, *Gadus morhua* L. *In* Early life history and recruitment in fish populations. *Edited by* R.C. Chambers and E.A. Trippel. Chapman and Hall Ltd., London, UK. pp. 251–278.
- Folkvord, A. 2005. Comparison of size-at-age of larval Atlantic cod (*Gadus morhua*) from different populations based on size- and temperature-dependent growth models. *Can. J. Fish. Aquat. Sci.* **62**: 1037–1052.
- Folkvord, A., Øiestad, V., and Kvenseseth, P.G. 1994. Growth patterns of three cohorts of Atlantic cod larvae (*Gadus morhua* L.) studied in a macrocosm. *ICES J. Mar. Sci.* **51**: 325–336.
- Folkvord, A., Blom, G., Johannessen, A., and Moksness, E. 2000. Growth-dependent age estimation in herring (*Clupea harengus* L.) larvae. *Fish. Res.* **46**: 91–103.
- Fonds, M., Cronie, R., Vethaak, A.D., and Van der Puyl, P. 1992. Metabolism, food consumption and growth of plaice (*Pleuronectes platessa*) and flounder (*Platichthys flesus*) in relation to fish size and temperature. *Neth. J. Sea Res.* **29**: 127–143.
- Gallego, A., and Heath, M. 1997. The effect of growth-dependent mortality, external environment and internal dynamics on larval fish otolith growth: an individual-based modelling approach. *J. Fish Biol.* **51**(Suppl. A): 121–134.
- Gallego, A., Heath, M.R., McKenzie, E., and Cargill, L.H. 1996. Environmentally induced short-term variability in the growth rates of larval herring. *Mar. Ecol. Prog. Ser.* **137**: 11–23.
- Govoni, J.J. 2005. Fisheries oceanography and the ecology of early life histories of fishes: a perspective over fifty years. *Sci. Mar.* **69**: 125–137.
- Grimm, V., and Railsback, S.F. 2005. Individual-based modeling and ecology. Princeton University Press, Princeton, N.J.
- Huston, M.A., and DeAngelis, D.L. 1987. Size bimodality in mono-specific populations: a critical review of potential mechanisms. *Am. Nat.* **129**: 678–707.
- Huston, M.A., DeAngelis, D.L., and Post, W. 1988. New computer models unify ecological theory. *Bioscience*, **38**: 682–691.
- Leggett, W.C., and Deblois, E. 1994. Recruitment in marine fishes — is it regulated by starvation and predation in the egg and larval stages. *Neth. J. Sea Res.* **32**: 119–134.
- Letcher, B.H., and Rice, J.A. 1997. Prey patchiness and larval fish growth and survival: inferences from an individual-based model. *Ecol. Model.* **95**: 29–43.
- Lough, R.G., Buckley, L.J., Werner, F.E., Quinlan, J.A., and Edwards, K.P. 2005. A general biophysical model of larval cod (*Gadus morhua*) growth applied to populations on Georges Bank. *Fish. Oceanogr.* **14**: 241–262.
- McGurk, M.D. 1986. Natural mortality of marine pelagic fish eggs and larvae: role of spatial patchiness. *Mar. Ecol. Prog. Ser.* **34**: 227–242.
- Otterlei, E., Nyhammer, G., Folkvord, A., and Stefansson, S.O. 1999. Temperature- and size-dependent growth of larval and early juvenile Atlantic cod (*Gadus morhua*): a comparative study of Norwegian coastal cod and northeast Arctic cod. *Can. J. Fish. Aquat. Sci.* **56**: 2099–2111.
- Oterå, H. 1992. Bias in calculating growth rates in cod (*Gadus morhua* L.) due to size selective growth and mortality. *J. Fish Biol.* **40**: 465–467.
- Pepin, P. 2004. Early life history studies of prey–predator interactions: quantifying the stochastic individual responses to environmental variability. *Can. J. Fish. Aquat. Sci.* **61**: 659–671.
- Pepin, P., Dower, J.F., and Benoet, H.P. 2001. The role of measurement error on the interpretation of otolith increment width in the study of growth in larval fish. *Can. J. Fish. Aquat. Sci.* **58**: 2204–2212.
- Peterson, I., and Wroblewski, J.S. 1984. Mortality rate of fishes in the pelagic ecosystem. *Can. J. Fish. Aquat. Sci.* **41**: 1117–1120.
- Pitchford, J.W., and Brindley, J. 2001. Prey patchiness, predator survival and fish recruitment. *Bull. Math. Biol.* **63**: 527–546.
- Pitchford, J.W., James, A., and Brindley, J. 2003. Optimal foraging in patchy turbulent environments. *Mar. Ecol. Prog. Ser.* **256**: 99–110.
- Pitchford, J.W., James, A., and Brindley, J. 2005. Quantifying the effects of individual and environmental variability in fish recruitment. *Fish. Oceanogr.* **14**: 156–160.
- Rice, J.A., Miller, T.J., Rose, K.A., Crowder, L.B., Marschall, E.A., Trebitz, A.S., and DeAngelis, D.L. 1993. Growth rate variation and larval survival: inferences from an individual-based size-dependent predation model. *Can. J. Fish. Aquat. Sci.* **50**: 133–142.
- Ricker, W.E. 1975. Computation and interpretation of biological statistics of fish populations. *Bull. Fish. Res. Board Can.* No. 191.
- Ripa, J., and Lundberg, P. 1996. Noise colour and the risk of population extinctions. *Proc. R. Soc. Lond. B*, **263**: 1751–1753.

Scheffer, M., Bavaco, J.M., Deangelis, D.L., Rose, K.A., and Vannes, E.H. 1995. Super-individuals: a simple solution for modeling large populations on an individual basis. *Ecol. Model.* **80**: 161–170.

Suthers, I.M., van der Meer, T., and Jorstad, K.E. 1999. Growth histories derived from otolith microstructure of three Norwegian

cod stocks co-reared in mesocosms: effect of initial size and prey size changes. *ICES J. Mar. Sci.* **56**: 658–672.

Tokarev, Y.N., Williams, R., and Piontkovski, S.A. 1998. Small-scale plankton patchiness in the Black Sea euphotic layer. *Hydrobiologia*, **376**: 363–367.

## Appendix A

**Table A1.** Symbols used for growth estimates in the individual-based model.

Symbols	Value and unit	Description
$DW_i$	mg dry weight	Dry weight
$SL_i$	mm	Standard length
$Ps_i$	—	Probability of survival
$N_i$	Individuals	The number of identical individual survivors represented by each super-individual. Initially $10^6$ and $10^8$ for cod- or herring-like species
$SGR_i$	%·day <sup>-1</sup>	Size-specific growth rate of larval Norwegian coastal cod ( <i>Gadus morhua</i> )
$g_i$ ( $g_{c,i}$ or $g_{h,i}$ )	day <sup>-1</sup>	Instantaneous growth rate for cod- or herring-like species
$\tilde{g}_{c,i}$	day <sup>-1</sup>	Instantaneous growth rate with environmental stochasticity for cod-like species
$e_i$		Error term
$\alpha$	[0, 1]	Autocorrelation coefficient
$\sigma$	[0, 0.7]	Standard deviation
$M_P(DW_i)$	day <sup>-1</sup>	Mortality rate dependent on body mass (Peterson and Wroblewski 1984)
$M_M(DW_i)$	day <sup>-1</sup>	Mortality rate dependent on body mass (McGurk 1986)
$M_f(SL_i)$	day <sup>-1</sup>	Predation rate increasing with standard length
$M_c(SL_i)$	week <sup>-1</sup>	Cannibalism predation rate dependent on relative standard length among the cohort
$g_{cs}$	day <sup>-1</sup>	Instantaneous population growth rate from cross-sectional data
$g_{lon}$	day <sup>-1</sup>	Instantaneous population growth rate from longitudinal data
$\overline{g}_{TMG}$	day <sup>-1</sup>	True mean growth rate of 60 DPH larvae
$\overline{DW}$	mg dry weight	Mean body mass of a cohort
$\epsilon_{cs}$	day <sup>-1</sup>	Bias from cross-sectional data
$\epsilon_{lon}$	day <sup>-1</sup>	Bias from longitudinal data